

To the theory of high-power gyrotrons with uptapered resonators

O. Dumbrajs¹ and G. S. Nusinovich²

¹*Institute of Solid State Physics, University of Latvia, Kengaraga Street 8, Riga LV-1063, Latvia*

²*Institute for Research in Electronics and Applied Physics, University of Maryland, College Park, Maryland 20742-3511, USA*

(Received 15 March 2010; accepted 15 April 2010; published online 20 May 2010)

In high-power gyrotrons it is desirable to combine an optimal resonator length with the optimal value of the resonator quality factor. In resonators with the constant radius of the central part, the possibilities of this combination are limited because the quality factor of the resonator sharply increases with its length. Therefore the attempts to increase the length for maximizing the efficiency leads to such increase in the quality factor which makes the optimal current too small. Resonators with slightly uptapered profiles offer more flexibility in this regard. In such resonators, one can separate optimization of the interaction length from optimization of the quality factor because the quality factor determined by diffractive losses can be reduced by increasing the angle of uptapering. In the present paper, these issues are analyzed by studying as a typical high-power 17 GHz gyrotron which is currently under development in Europe for ITER (<http://en.wikipedia.org/wiki/ITER>). The effect of a slight uptapering of the resonator wall on the efficiency enhancement and the purity of the radiation spectrum in the process of the gyrotron start-up and power modulation are studied. Results show that optimal modification of the shape of a slightly uptapered resonator may result in increasing the gyrotron power from 1052 to 1360 kW. © 2010 American Institute of Physics.

[doi:[10.1063/1.3425876](https://doi.org/10.1063/1.3425876)]

I. INTRODUCTION

One of the most critical issues in developing high-power gyrotrons for controlled fusion reactors is the gyrotron efficiency. The interaction efficiency of MW-level, long-pulse/cw millimeter-wave gyrotrons usually ranges from 30% to 35%; the wall-plug efficiency can be increased up to 45%–50% by using depressed collectors. For maximizing the interaction efficiency it is necessary, first, to design and fabricate an electron gun producing electron beam with high orbital-to-axial velocity ratio and low velocity spread. Second, it is necessary to optimize the resonator profile for providing (a) the axial structure of the resonator field favorable for efficient interaction with electrons gyrating in the guiding magnetic field and (b) realizing the quality factor (Q) yielding the optimal amplitude of high-frequency oscillations excited by an electron beam with given parameters.

In terms of the normalized parameters used in the general theory of the gyrotron,^{1–3} these two items mentioned above (the axial structure of the electromagnetic field and the resonator Q -factor) determine the normalized length and the normalized beam current parameter, respectively. In the simplest configuration of an open resonator with the constant radius and no reflection from the output end, these two factors, however, are not independent. The minimum diffractive Q -factor of such resonator is determined by its length L , or more exactly, by the ratio of the resonator length to the wavelength:^{4,3} $Q_D = 30(L/\lambda)^2$. A slight uptapering of a central part of such resonator shown in Fig. 1 offers more flexibility because it allows to simultaneously choose the resonator length optimal for the interaction efficiency and to adjust the diffractive Q for providing the optimal amplitude of the resonator field at given beam parameters and lowering the

density of Ohmic losses to the level affordable by the cooling conditions.

Some studies of the gyrotrons with slightly uptapered resonators were done in the past first in the USSR: In Ref. 5 the possibility to develop a frequency tunable gyrotron with a long slightly uptapered resonator was analyzed, while in Ref. 6 the effect of uptapering on the resonator diffractive Q -factor was studied. Later, some possibilities to use slightly uptapered resonators for optimizing the gyrotron operation were studied in Europe.^{7–10} In particular, in the cold cavity approximation it was found⁸ that tapering the midsection reduces Q substantially and shifts the maximum of the field profile toward the output end. This shift can help to slightly improve the efficiency because gradual increase in the wave amplitude near the entrance leads to a gentle modulation of electron energies and formation of a compact bunch, while then this electron bunch will be decelerated by the field of a large amplitude. In self-consistent calculations and in the experiments it was found¹⁰ that conical resonators seem to aggravate the problem of mode competition between the operating mode having one axial variation and modes having larger number of variations. Those studies were done for gyrotrons operating at relatively low-order modes, viz. the $TE_{0,3}$ (transverse-electric) mode.

In the present paper, we focus on such issues as the efficiency enhancement and the purity of the radiation spectrum in the process of the start-up and power modulation in the high-power gyrotron operating at a very high-order mode. The issue of power modulation is especially important for gyrotrons used for suppression of neoclassical tearing modes in large-scale tokamaks and stellarators. The spectral purity of gyrotron radiation is determined by the mode competition and the hard excitation of the high-efficiency mode.

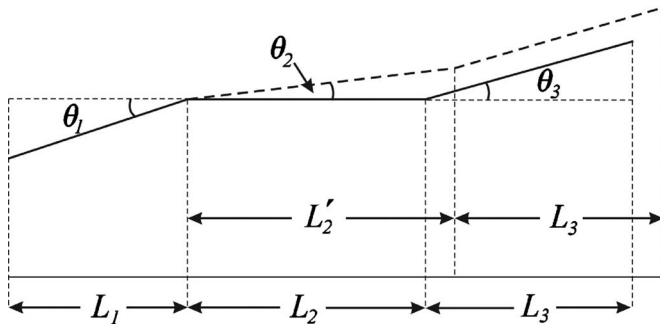


FIG. 1. Profiles of a standard resonator with the constant radius of its central part (solid lines) and that of a slightly uptapered resonator (dashed lines).

Both cause some hysteresis effects^{11,12} which are analyzed below.

In our study we analyze these issues in MW-class gyrotrons using the formalism described in detail in Ref. 11. The paper is organized as follows. In Sec. II we present results for the 170 GHz gyrotron (this frequency was chosen for gyrotrons in ITER). The section is subdivided into several subsections. First, we analyze several resonators of different lengths with different angles of uptapering and choose such angles that the diffractive Q -factors of the desired $TE_{32,09}$ mode of these resonators are practically the same. Then, we study a single-mode excitation of the operating $TE_{32,09}$ mode and show the effect of the changes in the resonator profile on the interaction efficiency. Lastly, we calculate the mode competition between the operating mode and two neighboring parasitic modes ($TE_{33,09}$ and $TE_{31,09}$ modes) in the process of start-up and power modulation. In Sec. III we discuss the results obtained and summarize our study.

II. THE EUROPEAN 170 GHz CYLINDRICAL CAVITY GYROTRON FOR ITER

Radiation from high-power gyrotrons will be used in ITER for electron cyclotron (EC) plasma heating and current drive (H&CD). In addition, the EC H&CD system is essential to control magnetohydrodynamics plasma instabilities such as the neoclassical tearing modes and sawteeth by driving localized current. It is foreseen to inject 20 MW of continuous 170 GHz power into the plasma by using gyrotrons as electromagnetic wave sources.¹³ Europe is developing the 2 MW coaxial cavity gyrotron for ITER. However, due to numerous delays and existing uncertainties related to coaxial gyrotrons, it has been decided to work in parallel on the 170 GHz 1 MW gyrotron with a cylindrical cavity as a fall-back solution.

It is planned that this gyrotron will be driven by an electron beam with the nominal current $I_{\text{opt}}=45$ A and the accelerating voltage $U_{\text{opt}}=79$ kV at which the pitch factor is $\alpha=1.3$. The operating mode is $TE_{32,09}$, which is quite similar to the $TE_{31,08}$ mode described in Ref. 13. The optimal electron beam radius providing the strongest coupling to this mode is $R_{el}=9.5$ mm. The cavity profile has been chosen as follows. The angles are: $\theta_1=2.5^\circ$, $\theta_2=0^\circ$, and $\theta_3=2.5^\circ$. The lengths of the sections are: $L_1=20$ mm, $L_2=14$ mm, and $L_3=20$ mm. The cavity has 4 mm rounding between the input taper and the straight section and 7 mm rounding between the straight section and the output taper, which effectively reduces the length of the straight section to 8.5 mm. The radius of the cavity (at the straight section) is $R_0=19.26$ mm. The cold frequency of the operating $TE_{32,09}$ mode is 170.027 GHz and the diffraction quality factor $Q=968$.

A. Cold cavity calculations

In our studies, to simplify simulations we remove roundings and consider four cavities with different middle section length and angle: **A** ($L_2=11$ mm, $\theta_2=0^\circ$), **B** ($L_2=14$ mm, $\theta_2=0.11^\circ$), **C** ($L_2=16$ mm, $\theta_2=0.145^\circ$), and **D** ($L_2=18$ mm, $\theta_2=0.16^\circ$). Here for the given length L_2 the angle θ_2 was chosen such that the resulting quality factors are approximately the same. The frequencies and quality factors obtained in the cold cavity approximation are summarized in Table I and the corresponding field profiles are shown in Fig. 2.

B. Self-consistent single-mode calculations

Self-consistent calculations done for a single operating mode in all four cavities under consideration revealed the optimal magnetic fields: $B=6.77$ T for cavity **A**, $B=6.75$ T for cavities **B** and **C**, and $B=6.74$ T for cavity **D**. (All calculations were done for an ideal beam, i.e., we neglected the electron velocity spread.) In Fig. 3 we show the dependence of the output power obtained in the four cavities on the accelerating voltage. It was assumed that, in the course of the voltage rise, the pitch-factor (orbital-to-axial velocity ratio) increases in accordance with the adiabatic theory of magnetron-type electron guns (see, e.g., Ref. 3) and in the range of voltages exceeding a half of the nominal voltage the beam current slightly increases as typical for such guns operating in the regime of temperature limited emission.

It should be noted that with increasing length and angle of the middle section of the cavity the maximum output

TABLE I. The frequencies and quality factors obtained in the cold cavity approximation.

Mode	A		B		C		D	
	F	Q	F	Q	F	Q	F	Q
33,09	173.109	1010	172.941	1014	172.849	999	172.775	1003
32,09	170.076	985	169.909	997	169.818	987	169.745	994
31,09	167.034	957	166.869	979	166.779	975	166.707	986

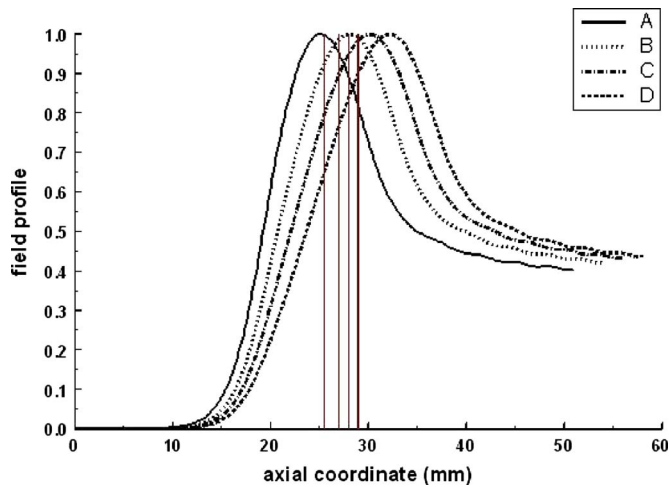


FIG. 2. (Color online) Axial profiles of the operating mode field in several resonators. Vertical lines mark the middle point of the cavity (25.5 mm for *A*, 27 mm for *B*, 28 mm for *C*, and 29 mm for *D*). Note that tapering shifts the maximum of the field profile toward the output end.

power increases. In particular, for the operating voltage $U=79$ kV the output power is 1052 kW in cavity *A*, 1222 kW in cavity *B*, 1360 kW in cavity *C*, and 1392 kW in cavity *D*.

It should also be noted that in a certain range of voltages the axial profile of the wave field calculated self-consistently strongly depends on the voltage, as was discussed in Ref. 14. In Fig. 4 we show the axial field profile for cavity *D* for four values of voltage. It is seen that at low voltages the field profile has two maxima (field profile with axial index two in the cold cavity approximation). With increasing voltage the profile approaches the shape with only one variation. This scenario can be explained by the relativistic changes in the electron cyclotron frequency with the voltage. At relatively low voltages, the beam line crosses the waveguide dispersion line far from cutoff, in the region of backward wave excitation of the mode with two variations. Then, as the voltage increases, the cyclotron frequency decreases, so the beam

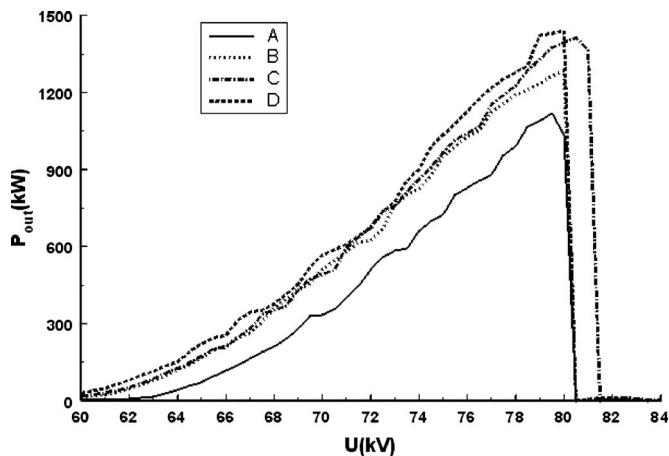


FIG. 3. Dependence of the output power on the beam voltage.

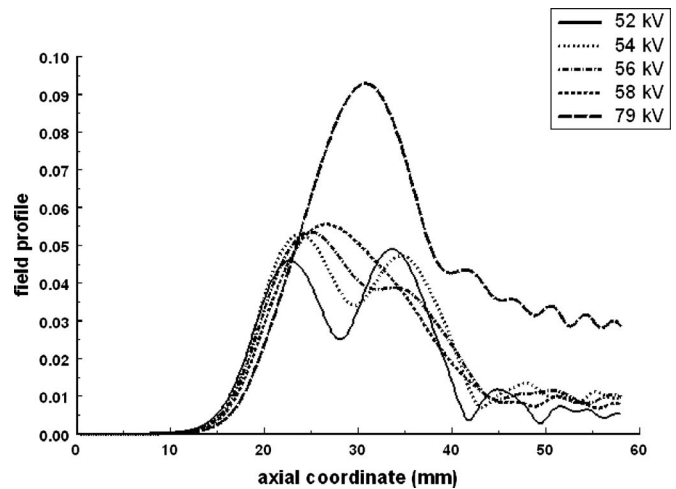


FIG. 4. Axial profile of the operating mode at several voltages. The field profile between 52 and 58 kV changes from two maxima to one maximum. Between 58 and 79 kV just the magnitude of the field profile is rising.

line moves down and the intersection takes place near cutoff, in the region of excitation of the mode with one axial variation.

This evolution of the axial structure of the resonator field with the voltage complicates the interpretation of the gyrotron operation. In gyrotrons with the fixed axial structure of the resonator field, in optimal regimes very often the hard excitation is observed (see, e.g., Refs. 3 and 12). In the hard excitation regime, as discussed in detail in Ref. 12, there are three equilibrium states, among which one is unstable, while two others are stable. This fact means that, depending on the history of evolution of gyrotron parameters, the device can operate in one of these two states, i.e., the device may exhibit a hysteresis. Interpretation of this phenomenon with the use of the polynomial dependence of the gyrotron source term on the mode intensity in the wave equation is given in Ref. 12. When the axial structure of the resonator field varies with the voltage the gyrotron operation in a desired mode can also exhibit some features of intermittency discussed in Ref. 14 which complicate the gyrotron operation even further, especially in the presence of parasitic modes.

C. Self-consistent multimode calculations

To study possible hysteresis effects caused by the mode interaction, we performed for each cavity two sets of calculations. First, we studied the gyrotron operation when the voltage increases from an initial value up to the nominal voltage $U=79$ kV and then returns back to the initial voltage. Second, to analyze the effect of voltage overshooting we considered the gyrotron operation when the voltage increases from an initial voltage up to $U=85$ kV and then returns back to the initial voltage. These voltage loops are especially important for gyrotrons developed for operation in power-modulated regimes, as discussed in Sec. I.

No overshooting. In the former case (no voltage overshooting), no hysteresis effects were observed in the cavities *A* and *B*, as shown in Fig. 5.

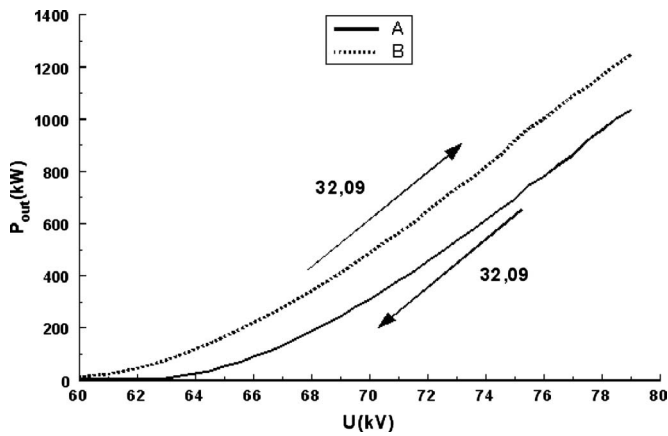


FIG. 5. Output power as a function of voltage in cavities *A* (solid line) and *B* (dotted line). Calculations were carried out from 60 to 79 kV and from 79 to 60 kV. No parasitic modes are excited, no hysteresis is seen.

However, cavities *C* and *D* exhibited more complicated behavior. In the cavity *C*, the hysteresis was observed due to excitation of a higher frequency parasitic mode $TE_{33,09}$, which was excited in the course of the voltage rise, but absent during the voltage fall, as shown in Fig. 6. This mode is absent during the voltage fall because this range of voltages corresponds to its hard self-excitation. The fact that during the voltage fall the operating mode remained stable in the range of voltages from 63 kV down to 52 kV should be attributed to the modification of its axial structure discussed above. The behavior of the gyrotron with the cavity *D* is even more complicated as shown in Figs. 7(a) and 7(b).

Results shown in Fig. 7(a) were obtained for the magnetic field of 6.74 T which in single-mode calculations was found to be optimal. However, in the presence of parasitic $TE_{31,09}$ and $TE_{33,09}$ modes, the gyrotron operation at the nominal voltage becomes unstable—the device exhibits the mode hopping from the operating to the lower-frequency

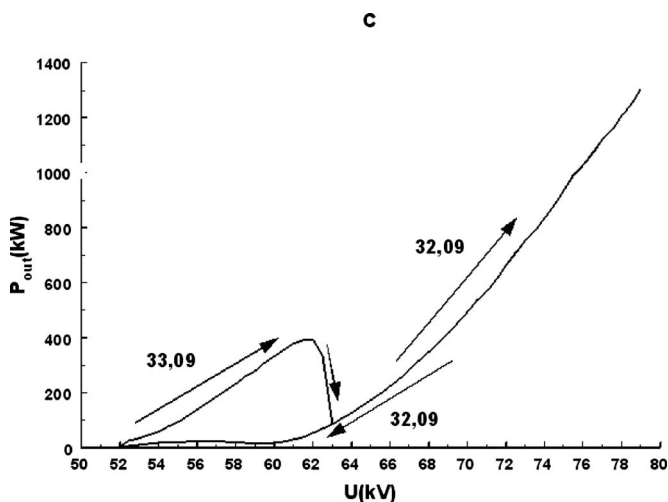
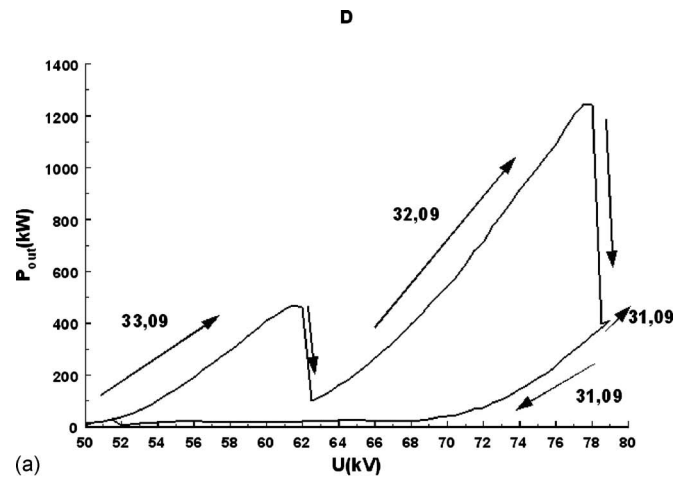
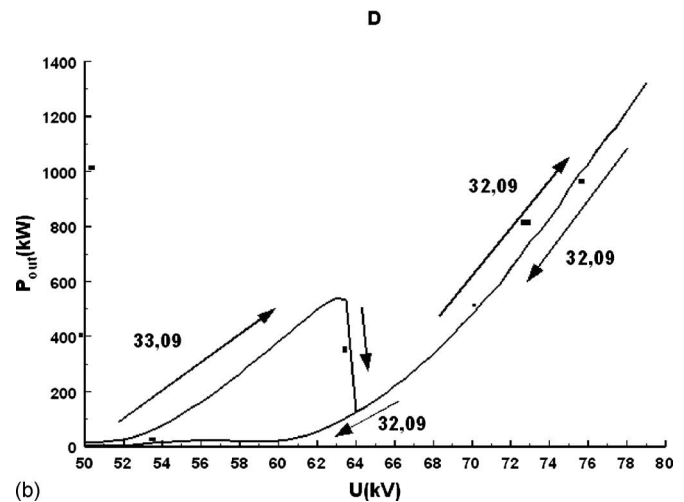


FIG. 6. Output power as a function of voltage. Calculations were carried out from 50 to 79 kV and from 79 to 50 kV. At low voltages, the parasitic $TE_{33,09}$ mode is excited. At 63 kV it is replaced by the operating $TE_{32,09}$ mode. Due to hysteresis when decreasing the voltage the operating mode survives until 52 kV. A clear hysteresis loop is seen.



(a)



(b)

FIG. 7. (a) Output power as a function of voltage. Here the magnetic field is equal to 6.74 T. Calculations were carried out from 50 to 79 kV and from 79 to 50 kV. At low voltages the parasitic $TE_{33,09}$ mode is excited. At 62.5 kV it is replaced by the operating $TE_{32,09}$ mode which survives until 78 kV where the parasitic $TE_{31,09}$ mode is excited. Due to hysteresis when decreasing the voltage this parasitic mode survives until 52 kV where the parasitic mode $TE_{33,09}$ reappears. A long hysteresis loop is observed and the operating $TE_{32,09}$ mode does not reappear at all. (b) Same as Fig. 7(a), but for 6.75 T.

parasitic $TE_{31,09}$ mode at 78 kV. Then, when the voltage drops, this parasitic mode oscillates at rather low power level until the voltage decreases down to about 51–52 kV, as shown in Fig. 7(a).

Then, the gyrotron switches from the low-frequency parasitic $TE_{31,09}$ mode to the high-frequency parasitic $TE_{33,09}$ mode which, in the course of the voltage rise, is replaced by the operating $TE_{32,09}$ mode at about 62 kV voltage. The maximum gyrotron power (1241 kW) in this case is reached at the voltage of 78 kV. This power is lower than the maximum power in the gyrotron with the cavity *C* (1360 kW). To avoid the mode hopping in the gyrotron with the cavity *D* at the nominal voltage, it is enough to increase the magnetic field from 6.74 to 6.75 T. Corresponding results are shown in Fig. 7(b).

Now the gyrotron remains stable at the nominal voltage and the hysteresis associated with the high-frequency parasitic $TE_{33,09}$ mode takes place at low (below 64 kV) only.

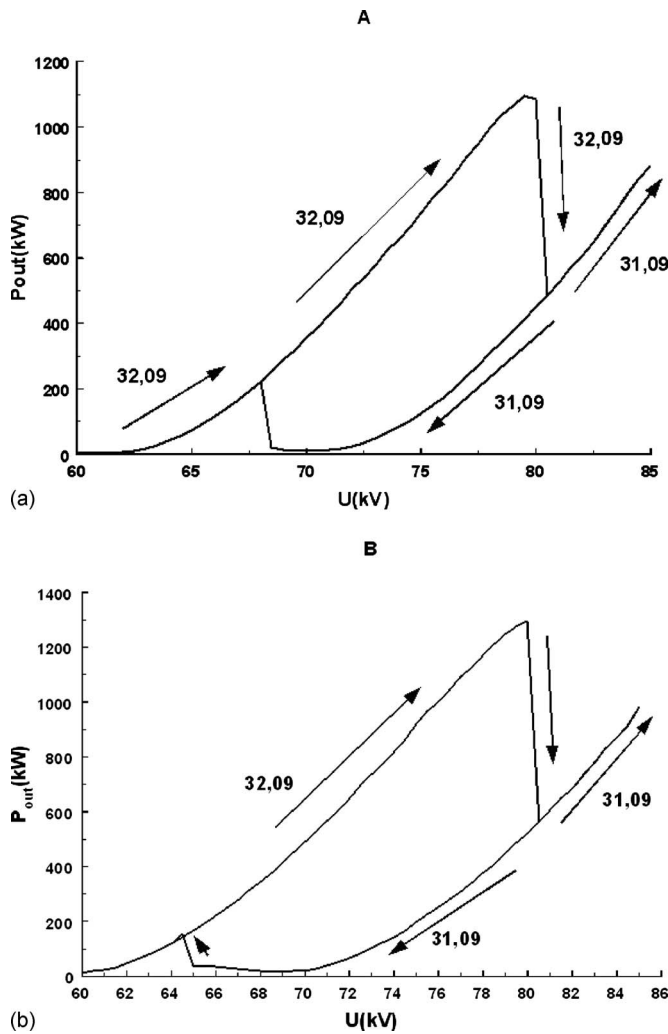


FIG. 8. (a) Output power as a function of voltage in a gyrotron with the cavity *A*. Calculations were carried out from 60 to 85 kV and from 85 to 60 kV. The parasitic $TE_{31,09}$ parasitic is excited at 80.5 kV. Due to the hysteresis, this mode survives when the voltage decreases until 64.5 kV where the operating $TE_{32,09}$ mode reappears. A clear hysteresis loop can be observed. (b) Output power as a function of voltage in a gyrotron with the cavity *B*. Calculations were carried out from 60 to 85 kV and from 85 to 60 kV. The parasitic $TE_{31,09}$ parasitic is excited at 80.5 kV. Due to the hysteresis, this mode survives when the voltage decreases until 64.5 kV where the operating $TE_{32,09}$ mode reappears. A clear hysteresis loop can be observed.

However, the maximum power at the nominal voltage is 1320 kW which is lower than in the gyrotron with the cavity *C*.

Overshooting. When the voltage increases up to 85 kV, which corresponds to the overshooting of about 7.6%, all gyrotrons exhibit mode hopping to the lower-frequency parasitic $TE_{31,09}$. There, the difference is only in their behavior during the voltage fall. The gyrotrons with the cavities *A* and *B*, as shown in Figs. 8(a) and 8(b), respectively, return back to the operating mode at the voltages either close to 70 kV [cavity *A* shown in Fig. 8(a)], or closer to 60 kV [cavity *B* shown in Fig. 8(b)].

In the case of the cavity *C* shown in Fig. 9, when the voltage falls the gyrotron switches from the low-frequency parasitic $TE_{31,09}$ mode to the high-frequency parasitic $TE_{33,09}$

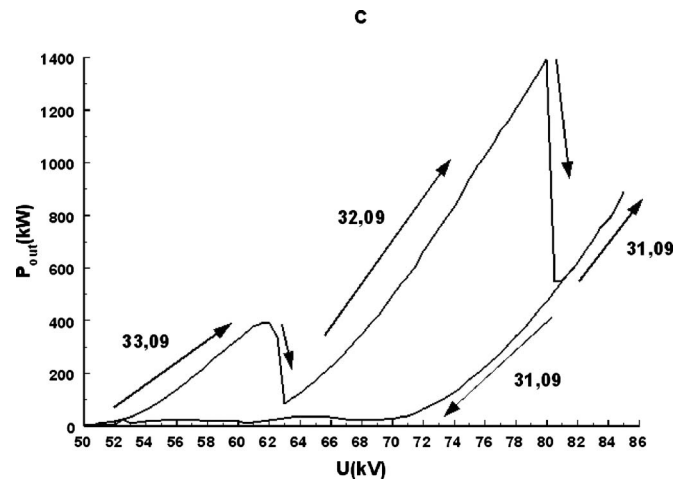


FIG. 9. Output power as a function of voltage. Calculations were carried out from 50 to 85 kV and from 85 to 50 kV. The parasitic $TE_{33,09}$ parasitic is excited at low voltages. At 63 kV it is replaced by the $TE_{32,09}$ operating mode which survives until 80 kV. At higher voltages the gyrotron oscillates in the parasitic $TE_{31,09}$ mode. Due to hysteresis when decreasing the voltage this mode survives until 53 kV where the parasitic $TE_{33,09}$ mode reappears. A huge hysteresis loop can be observed and the operating $TE_{32,09}$ does not reappear at all.

mode similar to the behavior of the gyrotron with cavity *D* in the absence of overshooting which was shown above in Fig. 7(a).

Results of our simulations with overshooting indicate that the operating mode remains stable only at rather small overshooting values, less than 0.6%. This imposes certain restrictions on the specifications of high-voltage supplies for such gyrotrons.

III. CONCLUSIONS

Our studies of gyrotrons with slightly tapered resonators allow us to draw several conclusions. First of all, slight up-tapering of such resonators can lead to the significant efficiency and power enhancement: 1360 kW with the 38% efficiency in the gyrotron with the cavity *C* versus 1052 kW with about 30% efficiency in the gyrotron with the cavity *A*. (Of course, more accurate efficiency data should be obtained with the account for the electron velocity spread.)

Second, there is an optimum cavity lengthening with the corresponding up-tapering. In the cases studied above it was shown that the optimal is the cavity *C* while the cavity *D* is too long. In so long cavities the gyrotron exhibits harder excitation and is less stable with respect to excitation of parasitic modes. In particular, it becomes unstable at the nominal voltage when the magnetic field is chosen optimal based on single-mode calculations.

With regard to possibilities to operate in power-modulated regimes we may conclude that in cavities with a constant or slightly increasing radius (cavities *A* and *B*), in principle, the power modulation up to 100% is possible, because we did not observe the hysteresis effects there. However, in stronger up-tapered cavities (cavities *C* and *D*) the power modulation is limited by possible mode hopping shown in Figs. 6 and 7(b). Note that, in practice, in order to

improve the reliability of gyrotron operation, experimentalists do not realize a 100% power modulation.¹⁵ It was also found that for stable operation with maximum power and efficiency the gyrotron high-voltage power supply should operate with rather small overshooting. (The last issue was also analyzed elsewhere.^{16,17})

ACKNOWLEDGMENTS

The work of the first author was supported by the Fusion for Energy (F4E) under grant Contract No. F4E-2008-GRT-08(PMS-H.CD)-01 and within the European Gyrotron Consortium (EGYC). EGYC is a collaboration among CRPP, Switzerland; KIT, Germany; HELLAS, Greece; CNR, Italy; ENEA, Italy. The views and opinions expressed herein only reflect the author's view. Fusion for Energy is not liable for any use that may be made of the information contained therein.

The work of the second author was supported by the Office of Fusion Energy of the U.S. Department of Energy.

¹A. V. Gaponov, M. I. Petelin, and V. K. Yulpatov, *Radiophys. Quantum Electron.* **10**, 794 (1967).

²B. G. Danly and R. J. Temkin, *Phys. Fluids* **29**, 561 (1986).

³G. S. Nusinovich, *Introduction to the Physics of Gyrotrons* (Johns Hopkins University Press, Baltimore, London, 2004), Chap. 4.

⁴S. N. Vlasov, G. M. Zhislin, I. M. Orlova, M. I. Petelin, and G. G. Rogacheva, *Radiophys. Quantum Electron.* **12**, 972 (1969).

⁵V. L. Bratman, S. L. Novozhilov, and M. I. Petelin, *Elektronn. Tekhn., Elektron., SVCh*, No. **11**, 46 (1976).

⁶V. E. Zapevalov and O. V. Malygin, *Izv. Vyssh. Uchebn. Zaved., Radiofiz.* **26**, 903 (1983).

⁷E. Borie and O. Dumbrajs, *Int. J. Electron.* **60**, 143 (1986).

⁸E. Borie, B. Jödicke, and O. Dumbrajs, *Int. J. Electron.* **61**, 735 (1986).

⁹E. Borie, B. Jödicke, H. Wenzelburger, and O. Dumbrajs, *Int. J. Electron.* **64**, 107 (1988).

¹⁰E. Borie, G. Gantenbein, B. Jödicke, G. Dammertz, O. Dumbrajs, T. Geist, G. Hochschild, M. Kunze, H.-U. Nickel, B. Piosczyk, and M. Thumm, *Int. J. Electron.* **72**, 687 (1992).

¹¹O. Dumbrajs, T. Idehara, Y. Iata, S. Mitsudo, I. Ogawa, and B. Piosczyk, *Phys. Plasmas* **10**, 1183 (2003).

¹²G. S. Nusinovich, O. V. Sinitsyn, L. Velikovich, M. Yeddulla, T. M. Antonsen, Jr., A. N. Vlasov, S. R. Cauffman, and K. Felch, *IEEE Trans. Plasma Sci.* **32**, 841 (2004).

¹³K. Sakamoto, A. Kasugai, K. Kajiwara, K. Takahashi, Y. Oda, K. Hayashi, and N. Kobayashi, *Nucl. Fusion* **49**, 095019 (2009).

¹⁴G. S. Nusinovich, M. Yeddulla, T. M. Antonsen, Jr., and A. N. Vlasov, *Phys. Rev. Lett.* **96**, 125101 (2006).

¹⁵J. Lohr (personal communication).

¹⁶M. Yu. Glyavin, *Elektronnaya Tekhnika, Ser. I, Elektron. SVCh* **3**, 3 (1990).

¹⁷G. S. Nusinovich, A. N. Vlasov, T. M. Antonsen, Jr., J. Lohr, B. G. Danly, and J.-P. Hogge, *Phys. Plasmas* **15**, 103101 (2008).